Acta Cryst. (1964). **17**, 1312

Study of Phase Transformations During Calcination of Aluminum Hydroxides by Selected Area Electron Diffraction

B. C. LIPPENS* AND J. H. DE BOER

Department of Chemical Technology, Technological University, Delft, The Netherlands

(*Received* 29 *July* 1963)

Bayerite, β-Al(OH)$_3$, and boehmite, γ-AlOOH, both with crystallite sizes of some tenths of a micron, were used for this investigation.

The transformation of bayerite to η-alumina and of boehmite to γ- and δ-alumina showed a strict pseudomorphosis. η- and γ-alumina have spinel lattices that differ in disorder: η-alumina has a strong one-dimensional disorder of the cubic close-packed stacking; for γ-alumina the oxygen sublattice is fairly well ordered, whereas the tetrahedral Al lattice is strongly disordered.

The crystallographic texture of η- and γ-alumina could be related to their microporous texture and this in its turn to the length of the OH bonds in the hydroxides.

The formation of the well ordered super spinel structure δ-Al$_2$O$_3$ is suppressed by obstructing the diffusion of the Al ions either by the surface of numerous pores (η-alumina from bayerite or γ-alumina from gelatinous boehmite) or by incorporating large ions such as Na ions (γ-alumina from crystalline boehmite). In these cases the disordered spinel type aluminas are transformed at a high temperature to θ- and α-Al$_2$O$_3$ by complete recrystallization to small particles which still have some preferred orientation.

Introduction

Aluminas used as catalysts or as carriers for catalysts are generally obtained by calcining aluminum hydroxides at a certain temperature. The crystallographic structure and texture and the microporous texture of the aluminas largely determine the properties of their surfaces. In other papers (de Boer & Lippens, 1964*a*, *b*) we have described the microporous texture of various aluminas as shown by nitrogen and lauric acid adsorption measurements. In the present paper the crystallographic structure and texture of the aluminas derived from two crystalline aluminum hydroxides, bayerite (β-Al(OH)$_3$) and boehmite (γ-AlOOH), are described. We used the selected area electron diffraction technique as both hydroxides have been obtained only in a very finely divided state, the particle size being of the order of some tenths of a micron and therefore unsuitable for single-crystal X-ray investigations. We did not intend to obtain exact information on the atom parameters, as we were mainly interested in the pseudomorphosis relations and the principal features of the defect structure of the aluminas.

Starting materials

Bayerite was obtained by Schmäh's (1946) method by the reaction of amalgamated aluminum with water at room temperature.

Boehmite was obtained by heating a commercial gibbsite for 6 hr in an excess of liquid water at 250 °C in an autoclave. More detailed information concerning preparation methods is given elsewhere (Lippens, 1961).

Diffraction records

X-ray diffraction diagrams were made with a standard Philips X-ray diffractometer and proportional counter, Cu $K\alpha$ radiation being used. The electron diffraction patterns were obtained with the Elmiskop I (Siemens and Halske), which is provided with facilities for selected area electron diffraction and dark field illumination. The accelerating voltage used was 80 kV. A drawback is that manipulation of the objects is very limited. As a consequence of the preparation technique the sample particles generally possessed a certain preferred orientation, so for the greater part only one crystal zone of the samples could be observed.

Results of X-ray powder methods

The hydroxides

The powder diagram of bayerite can be indexed completely, assuming an orthorhombic (nearly hexagonal) unit cell with the axes:

$$a=8{\cdot}764,\ b=5{\cdot}061,\ c=4{\cdot}713\ \text{Å}\ .$$

The unit cell contains 4 Al atoms and 12 OH groups; it consists of two closest-packed layers of OH groups separated by a layer of Al atoms in octahedral positions. Each unit cell contains two vacant octahedral positions, each of which is surrounded by 6 Al atoms.

---

* Present address: Laboratory for Inorganic Chemistry, Technological University, Eindhoven, The Netherlands.

The bonding between these double layers is due to hydrogen bonds of the OH groups.

Boehmite has also an orthorhombic unit cell with the axes:

$$a = 2{\cdot}861,\ b = 3{\cdot}696,\ c = 12{\cdot}233\ \text{Å}\,.$$

It consists of chains of AlO_6 octahedra giving double molecules

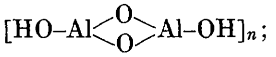

$$[\mathrm{HO{-}Al}\overset{\mathrm{O}}{\underset{\mathrm{O}}{<>}}\mathrm{Al{-}OH}]_n;$$

the chains are parallel, forming layers with the OH groups outside. Again the bonding between these layers is due to hydrogen bonds.

It should be remarked that the notation of the axes used here deviates from that in the literature; we have uniformly placed the *c* axis perpendicular to the cleavage plane, which is formed by the layers described. A more detailed description of the probable structure of the hydroxides is given elsewhere (Lippens, 1961).

Characterization of the aluminas

The only modification of Al_2O_3 which does not give trouble in characterization is the stable α-Al_2O_3 (corundum). Of the numerous aluminas that are described in the literature, four are found during the dehydration of boehmite and bayerite, *viz.* γ and η at low temperature and δ and θ at high temperature. Much confusion exists in this respect, so we thought it useful to indicate the main differences between

Table 1. *X-ray powder diffraction data of* γ- *and* η-*alumina*

γ-Alumina			η-Alumina			Spinel
2θ	*d*	*I*	2θ	*d*	*I*	*hkl*
19·3	4·6	12	19·4	4·57	16	111
32·3	2·77	25	32·4	2·76	33	220
37·49	2·397	60	37·52	2·395	70	311
39·42	2·284	33	39·41	2·284	36	222
45·54	1·990	65	45·80	1·980	70	400
46·38	1·956		—	—	—	—
60·90	1·520	15	60·94	1·519	16	333/511
66·38	1·407	100	66·95	1·396	100	440
67·04	1·395		—	—	—	—

Table 2. *X-ray powder-diffraction data of* δ- *and* θ-*alumina*

The lines indicated by (α) have a varying intensity for different samples; they must be ascribed to small amounts of α-Al_2O_3

δ-Alumina			
2θ	*d*	*I*	*hkl*
11·6	7·6	2	101
13·8	6·4	2	102/004
16·0	5·53	2	111
17·35	5·10	5	112
19·40	4·57	8	113
21·80	4·07	8	114/105
24·65	3·61	2	115
27·60	3·23	2	116
29·25	3·05	2	107/214/205
31·01	2·881	5	117
32·80	2·728	20	222
34·45	2·601	15	302/118
36·50	2·460	40	312
37·40	2·402	10	313
38·87	2·315	5	314/305
39·50	2·279	25	226
41·78	2·160	3	11·10
45·64	1·986	50	400
46·45	1·953	25	00·12
47·46	1·914	8	318
49·87	1·827	3	333
50·36	1·810	5	319/22·10
56·47	1·628	5	426/31·11
57·40	1·604	3	11·14
60·11	1·538	5	513
61·02	1·517	10	339/11·15
63·88	1·456	5	523/516/20·15
66·38	1·407	35	440
66·98	1·396	65	40·12

θ-Alumina			
2θ	*d*	*I*	
16·20	5·47	5	
17·50	5·06	3	
19·42	4·57	10	
22·20	4·00	3	
25·48	3·493	5	(α)
31·26	2·859	60	
32·76	2·731	100	
35·06	2·557	10	(α)
36·46	2·462	80	
37·67	2·386	5	(α)
38·88	2·314	40	
39·78	2·264	30	
43·20	2·092	5	(α)
44·64	2·028	80	
47·50	1·913	40	
50·66	1·800	5	
51·65	1·768	5	(α)
57·04	1·613	5	(α)
60·11	1·538	20	
62·54	1·484	20	
63·88	1·456	20	
65·22	1·429	10	
66·37	1·407	30	
67·18	1·392	100	
68·14	1·375	3	(α)

these types of alumina. As regards the notation we have based ourselves on the observations made by Tertian & Papée (1958).

The powder patterns of γ- and η-alumina are very similar. Table 1 gives the spacings and the integrated intensities. Owing to the very diffuse character of the pattern (the sharpest bands having a half maximum breadth of about 2° in 2θ) the intensities are only approximate. The patterns can be indexed according to a spinel lattice. The principal differences between γ- and η-alumina are:

(*a*) The 111 reflexion of γ-alumina is very diffuse, while that of η-alumina is sharp with a broadened base.

(*b*) The 400 and the 440 reflexions of γ-alumina are clearly doubled, while those of η-alumina have only an asymmetrical profile and a broadened base.

The powder patterns of δ- and θ-alumina consist of a great number of fairly sharp lines; δ-alumina especially gives many weak reflexions with spacings larger than 4 Å (Table 2).

The main differences between the two modifications are:

(*a*) The intensities of the peaks in the region of spacings between 3·0 and 2·2 Å (30 to 40° 2θ) are higher for θ- than for δ-alumina.

(*b*) In the region of spacings of 2·0 Å we find two peaks with spacings of 2·03 and 1·91 Å for θ- and three peaks with spacings of 1·99, 1·95 and 1·91 Å for δ-alumina.

Dehydration sequences of the hydroxides

Using the characterization mentioned above we found the following dehydration sequences:

Fig. 1. Diffraction pattern of conical bayerite particle.

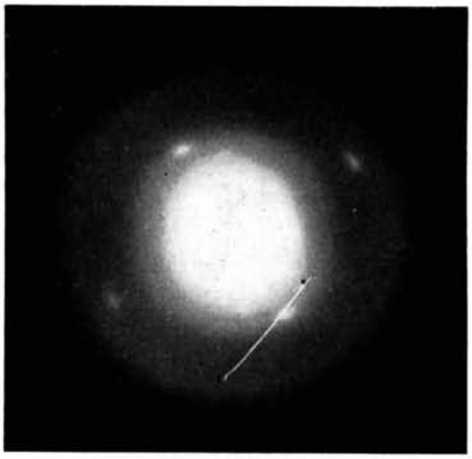

Fig. 2. Diffraction pattern of conical bayerite particle after heating to 400 °C.

Fig. 3. Diffraction pattern of platelet of bayerite.

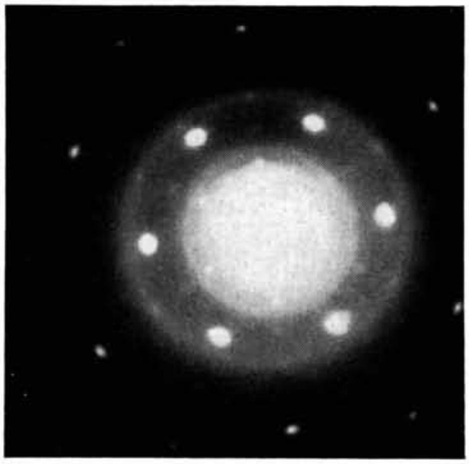

Fig. 4. Diffraction pattern of platelet of bayerite after heating to 400 °C.

$$\text{Boehmite} \xrightarrow{450\ ^\circ\text{C}} \gamma \xrightarrow{750\ ^\circ\text{C}} \delta \xrightarrow{1000\ ^\circ\text{C}} \theta + \alpha \xrightarrow{1200\ ^\circ\text{C}} \alpha\text{-Al}_2\text{O}_3$$

$$\text{Bayerite} \xrightarrow{230\ ^\circ\text{C}} \eta \xrightarrow{850\ ^\circ\text{C}} \theta \xrightarrow{1200\ ^\circ\text{C}} \alpha\text{-Al}_2\text{O}_3\ .$$

The temperatures given here are only approximate; so the conversion rate of well-crystallized boehmite to γ-alumina is still extremely low at 400 °C; poorly crystallized boehmite can be transformed to γ-alumina at temperatures below 350 °C. The same holds for some other conversions.

Under the influence of intergranular hydrothermal conditions a small part of the bayerite is converted into well-crystallized boehmite. The amount of boehmite formed, however, is very low and is neglected for the dehydration scheme.

The indexing of the diagram of δ-alumina is based on the assumption of a super cell of spinel consisting of three spinel blocks on each other, as was done by van Oosterhout & Rooymans (1958) for γ-Fe_2O_3. With $a=b=7{\cdot}943$ and $c=23{\cdot}50$ Å a good solution was obtained. From electron diffraction observations it appeared that this assumption is correct.

Pseudomorphosis relations

Bayerite

The sample principally consists of conical or hourglass shaped particles (*cf.* Kohlschütter, Beutler, Sprenger & Berlin, 1931; Watson, Parsons, Vallejo-Freire & Santos, 1955; Moscou & van der Vlies, 1959), which are built up from a great number of platelets approximately perpendicular to the longitudinal direction of the somatoids. Sometimes some very thin platelets are found.

The diffraction patterns of the conical or hour-glass shaped particles generally show only one single row of spots through the centre, corresponding to 00*l*-reflexions (repetition distance 4·7 Å). The direction of this row coincides approximately with the longitudinal direction of the somatoids. Sometimes some rows of 0*kl* reflexions are also observed (Fig. 1).

After heating, such a particle gives a diffraction pattern as shown in Fig. 2. The reflexions observed belong to the $[01\bar{1}]$ zone of the spinel (Fig. 5).

Fig. 3 gives the diffraction pattern of a very thin platelet of bayerite. It shows the [001] zone of bayerite.

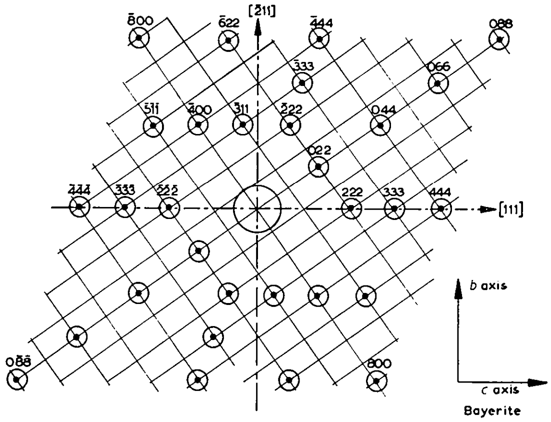

Fig. 5. Indices of diffraction pattern of Fig. 2. Circles with black dots indicate observed reflexions.

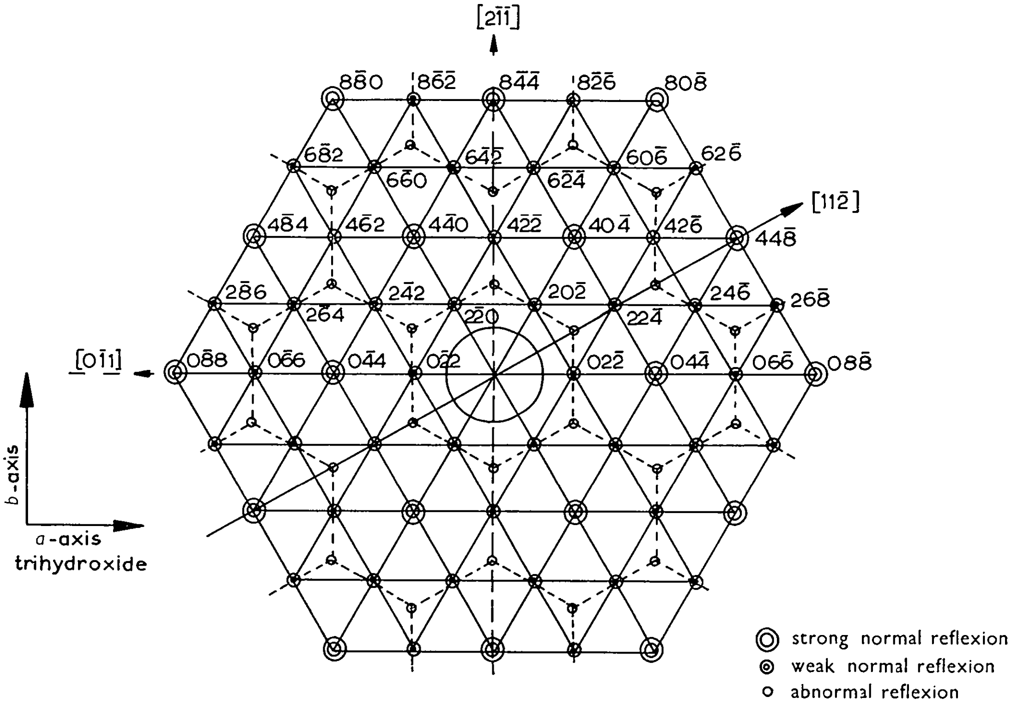

Fig. 6. Indices of diffraction pattern of Fig. 4.

Table 3. *Pseudomorphosis relations of bayerite and η-alumina*

Bayerite			Spinel		
Axis	Platelets	Cones	Axis	d	$\Delta l/l$
a	$8{\cdot}66 = 3 \times 2{\cdot}89$	—	$[01\bar{1}]$	$5{\cdot}58 = 2 \times 2{\cdot}79$	$-3{\cdot}3\%$
b	5·00	5·00	$[\bar{2}11]$	$3{\cdot}24 = \frac{2}{3} \times 4{\cdot}86$	$-2{\cdot}9\%$
c	—	4·72	$[111]$	4·57	-52%*

* Two unit cells of bayerite containing 4 close-packed OH layers parallel to the cleavage plane form two close-packed O layers in the spinel lattice by loss of water during dehydration, so $2 \times 4{\cdot}72$ Å in the bayerite lattice corresponds to 4·57 Å in the spinel lattice giving a $\Delta l/l$ of 52%.

After heating, the pattern given in Fig. 4 is obtained, which shows the [111] zone of the spinel (Fig. 6). A number of abnormal reflexions is observed, which can only be indexed with fractional numbers instead of integers, *e.g.* $\frac{4}{3}\frac{4}{3}\,-\frac{8}{3}$. Such reflexions are observed more often in electron diffraction patterns; they originate from certain lattice defects, as will be discussed later.

Comparing the patterns of the heated samples with those of the hydroxide particles, we get the pseudomorphosis relations as given in Table 3.

From the diffraction patterns the ratio of the a and the c axes of the η-alumina spinel can be calculated; it varied between 0·985 and 0·993 for the various records. So apparently the η-alumina spinel is somewhat tetragonally deformed.

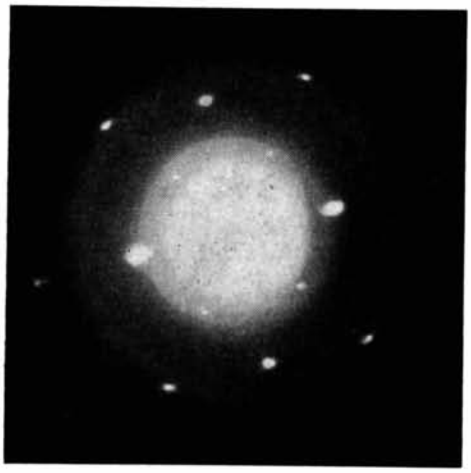

Fig. 7. Diffraction pattern of a boehmite single crystal.

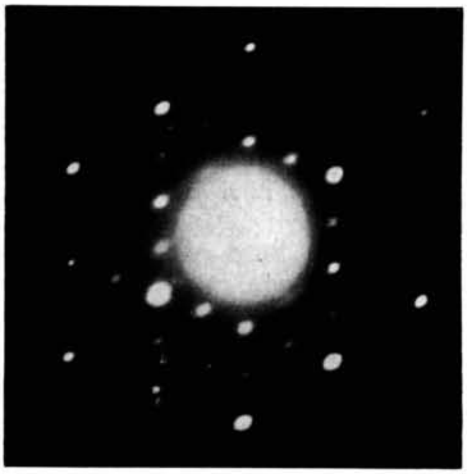

Fig. 8. Diffraction pattern of γ-alumina from a boehmite single crystal.

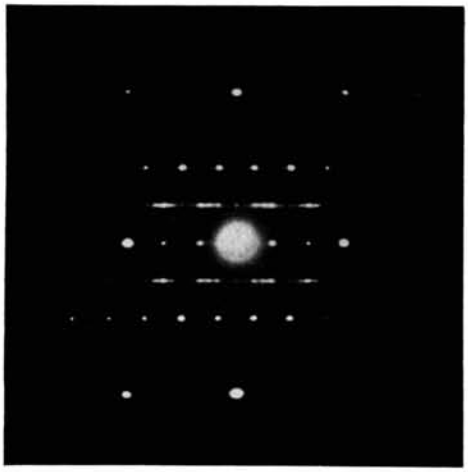

Fig. 9. Diffraction pattern of δ-alumina from a boehmite single crystal.

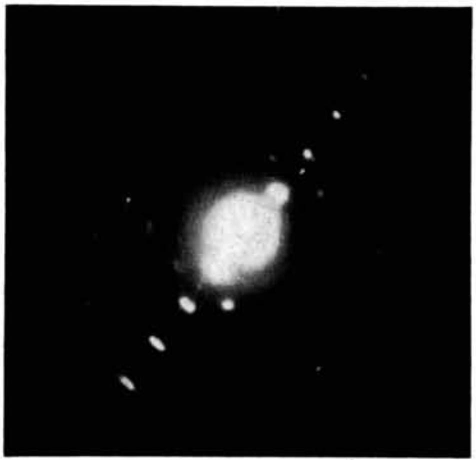

Fig. 10. Diffraction pattern of a bayerite particle after heating to 980 °C.

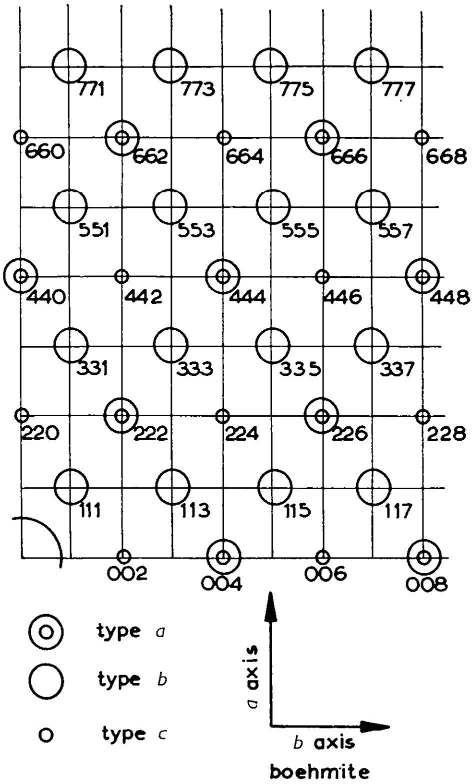

Fig. 11. Indices of diffraction pattern of Fig. 8.

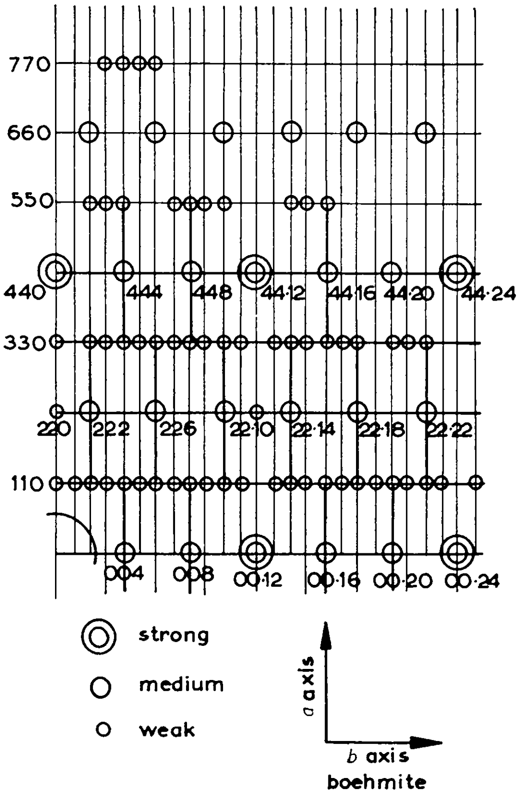

Fig. 12. Indices of diffraction pattern of Fig. 9.

Boehmite

Figs. 7, 8 and 9 give the results of the heating of boehmite. The crystals of this sample that were suited for selected area diffraction are rhombus-shaped and all lay with the plane of the rhombus on the supporting film, *i.e.* perpendicular to the beam. From Fig. 7 it follows that the a (2·86 Å) and the b (3·69 Å) axis of the boehmite lattice are lying parallel to the supporting film. The c axis is then parallel to the incident beam and the cleavage plane parallel to the basis and the top of the crystal. The side planes are apparently formed by $\{110\}$ planes.

On heating at about 500 °C a pattern of γ-alumina is obtained (Fig. 8), which is indexed in Fig. 11; the reflexions belong to the $[1\bar{1}0]$ zone of the spinel lattice. Table 4 gives the pseudomorphosis relations. These relations are the same as those observed by Saalfeld (1958) on boehmite crystals obtained by pseudomorphous conversion of gibbsite single crystals and analogous to those stated by van Oosterhout (1960) for the transformation of lepidocrocite (γ-FeOOH) into γ-Fe_2O_3. The γ-alumina again possesses a tetragonal lattice with $c/a = 0·983$ to 0·987 for the various records.

On heating the boehmite sample at a temperature of 850 °C, when δ-alumina is formed, a diffraction pattern is obtained as shown in Fig. 9. The strong recrystallization clearly appears from the sharpening of the diffraction spots. Fig. 12 gives the indexed diagram. The numerous hhl reflexions with odd h confirm the presence of a long c axis of 23·5 Å, as we found already from the X-ray powder diagram. From the absence of $00l$ reflexions with $l \neq 4n$ a fourfold screw axis follows in the $\mathbf{c}$ direction, which was also found by van Oosterhout and Rooymans (1958) for γ-Fe_2O_3.

Table 4. *Pseudomorphosis relations of boehmite and γ-alumina*

Boehmite		Spinel		
Axis	d	Axis	d	$\Delta l/l$
a	2·85	[110]	$5·63 = 2 \times 2·81$	−1·2%
b	3·69	[001]	$7·82 = 2 \times 3·91$	+6·0%
c	12·23	$[1\bar{1}0]$	5·63	−31%*

* One unit cell of boehmite (12·24 Å) containing four O and four OH layers parallel to the cleavage plane form six O layers in the spinel lattice by loss of water during dehydration; these six O layers in *CDCD* stacking take in $\frac{6}{4} \times 5·63$ Å = 8·45 Å corresponding to a $\Delta l/l$ of 31%.

The crystallographic texture of the aluminas

In the diffraction patterns of platelets of bayerite after transformation to η-alumina we noticed a

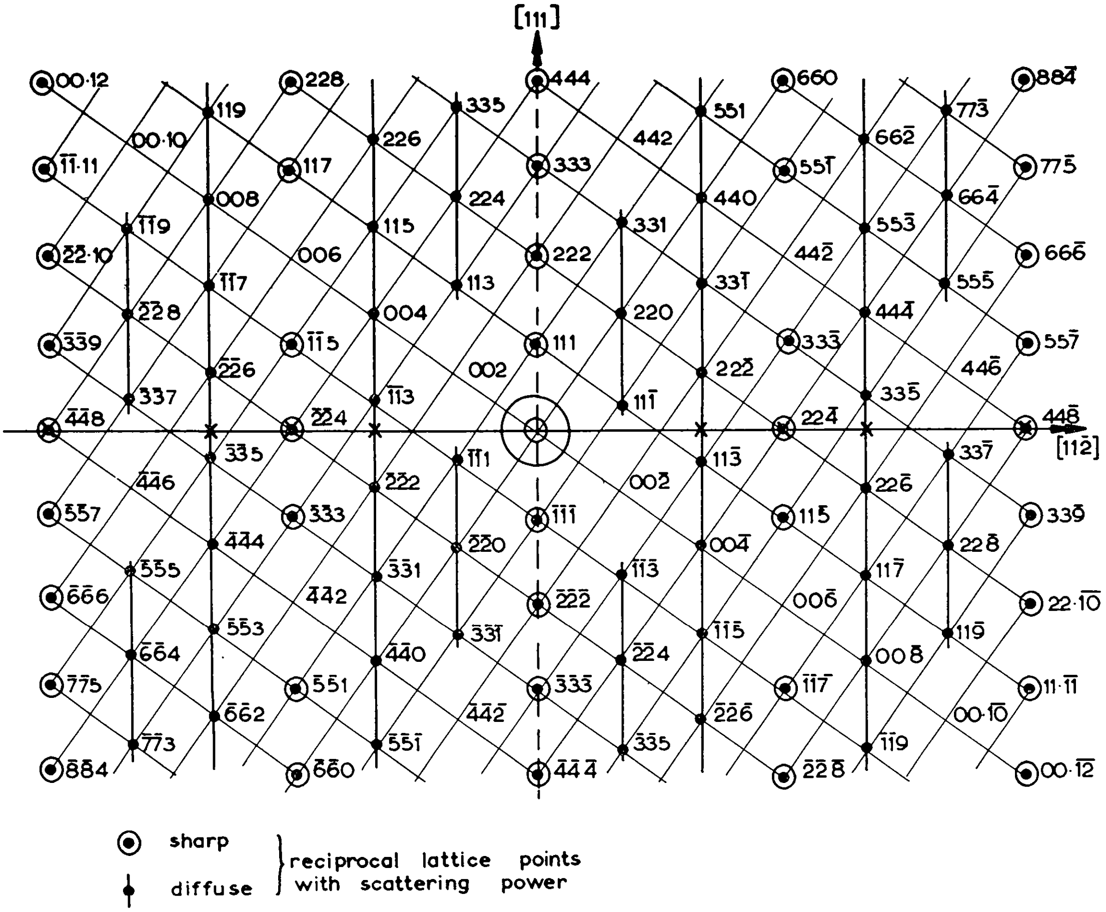

Fig. 13. Cross-section through the reciprocal lattice of η-alumina perpendicular to $[1\bar{1}0]$. Crosses indicate observed reflexions.

number of reflexions which could not be indexed with integers. For the rest these reflexions can be distinguished from the others neither in appearance nor in intensity. In the powder diagrams they do not occur. Fig. 13 gives the cross-section through the reciprocal lattice of the spinel perpendicular to the $[1\bar{1}0]$ direction and the [111] axis parallel to the incident beam as it was during recording. It appears that the abnormal reflexions can be explained by assuming a suitable extension of the reciprocal lattice 'points', arising from certain lattice defects. The trihydroxide lattice itself is fairly regular, the reflexions are sharp and abnormal reflexions do not occur. During the transformation into η-alumina the originally hexagonal oxygen arrangement (layer sequence *AB AB AB*) is converted into the cubic arrangement *ABC ABC ABC* by loss of nearly half of the total number of oxygen atoms as water molecules. This implies an almost complete breaking down and rebuilding of the oxygen sublattice *via* the cleavage plane (the (001) plane) of the hydroxide, which then becomes the (111) plane of the spinel. Deviations from the regular cubic arrangement can occur now as *e.g. ABCACABABCBC etc.* Jagodzinski & Laves (1948) and Cowley & Rees (1958) have shown that in the case of complete randomness of such a stacking only for reflexions for which $h-2k+l=3n$ will there be a sharp maximum of scattering power. The other reflexions are replaced by continuous lines of scattering power parallel to the [111] axis. If the degree of randomness is smaller these continuous lines also occur, but with maxima and minima of scattering power corresponding to those of the ideal reciprocal lattice.

The occurrence of continuous lines parallel to the [111] direction was also demonstrated by Cowley (1953) in an oriented specimen of alumina obtained from the oxidation of aluminum foil.

The electron diffraction patterns of γ-alumina obtained from boehmite differ considerably from those of η-alumina from bayerite.

In Fig. 8 giving the [110] zone we can distinguish three types of reflexion, *viz.*:

Type *a* with sharp maximum and broadened base; these are reflexions of which the indices, after division by two, still belong to a face-centred lattice.

Type *b* reflexions without sharp maximum, length about twice the breadth; they are all reflexions with odd indices.

Type *c* reflexions without sharp maximum, length more than three times the breadth; these reflexions have even indices, which, upon division by two, do not belong any more to a face-centered lattice.

Calculating the systematic extinctions and structure factors for the ideal spinel lattice, it appears that the type *a* reflexions originate from the oxygen sublattice and the cation sublattice together, the type *b* reflexions from the total cation sublattice, the contributions from the oxygen sublattice being negligible. Finally the type *c* reflexions originate only from the cations in *tetra*hedral positions, the contributions from the oxygen sublattice and the cations in *octa*hedral positions being negligible.

If we consider the possible mechanism of the dehydration of boehmite we notice that only half of the oxygen layers are included in the dehydration (unlike the dehydration of the trihydroxides, where all oxygen layers contribute). Only the layers formed by the OH groups are broken down, the O layers remaining two and two intact. These latter layers form the skeleton on which the spinel lattice will be rebuilt.

In the orientation which the spinel lattice takes in by pseudomorphosis we find two oxygen layers with a different cation occupation (*C* and *D*, Fig. 14). The stacking of these layers on each other is, apart from the cation arrangement, only possible in one way, *viz. CD CD CD etc.* (*Cf.* Sasvári & Zalai, 1957). Consequently the oxygen lattice of γ-alumina from boehmite will have a much better ordering than that of η-alumina from the trihydroxides. In agreement with this all reflexions in which the oxygen sublattice plays an important role are of type *a*.

To obtain the spinel lattice $21\frac{1}{3}$ aluminum atoms and $2\frac{2}{3}$ vacant sites have to be distributed over the octahedral and tetrahedral positions. Whether the vacant sites will occur in octahedral or in tetrahedral positions, the greatest disorder is to be expected for the atoms in tetrahedral positions.

Those reflexions which mainly originate from the tetrahedral lattice will possess the strongest diffuse character. They all belong to type *c*.

The disorder of the tetrahedral lattice will also explain why reflexions such as 002 and 006 may occur, which are forbidden in the ideal spinel pattern and which also belong to type *c*.

In δ-alumina the perfect ordering of the lattice is not yet complete, as follows from the presence of weak continuous lines in the pattern (indicated in Fig. 12 by thicker lines). Especially in the direction of the long *c* axis some disorder is still present.

Comparison of X-ray and electron diffraction results

The X-ray powder diagram of η-alumina consists of broadened lines, often with a fairly sharp top. Only part of the coinciding reflexions satisfies the condition for sharp reflexions $h-2k+l=3n$. This is clear especially in the case of the 111 reflexion, which is

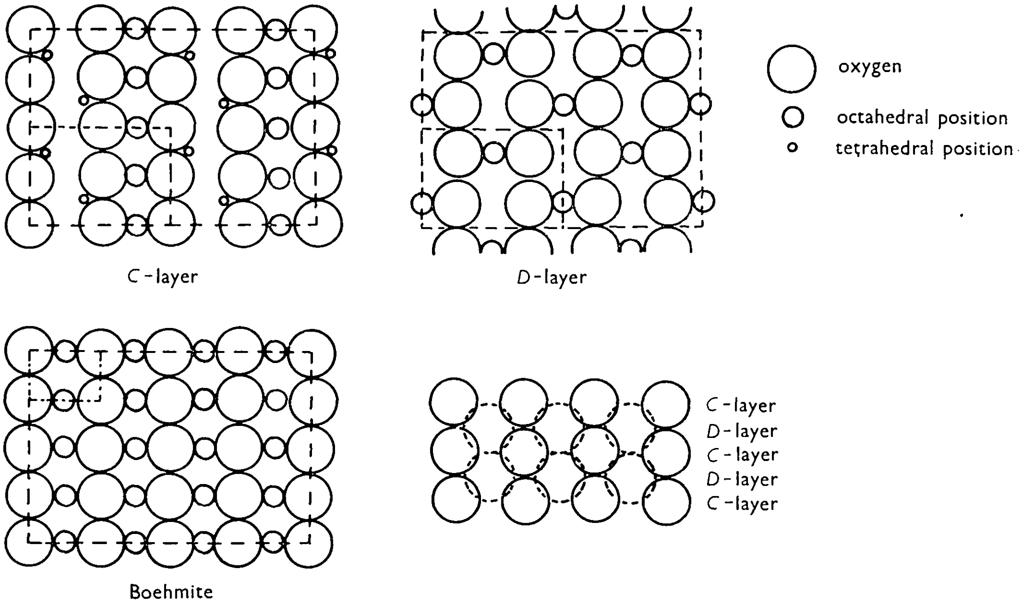

Fig. 14. Cation positions in the spinel lattice; oxygen layers parallel to (110) planes.

characteristic of η-alumina. The intensity of the sharp portion of this line is about one fourth of the total intensity, which is in agreement with the coincidence of the four 111 reflexions of which only one is sharp.

For γ-alumina the reflexions to whose intensity the oxygen sublattice contributes to a large degree, are fairly sharp (compare type *a*); all other reflexions are broad. The 220 reflexion especially is very diffuse (type *c*).

The tetragonal character of η-alumina is less pronounced than that of γ-alumina and finds expression only in the asymmetry of the 400 and 440 reflexions instead of a clear line-doubling. The changes of the lengths of the axes of bayerite parallel to the cleavage plane during the transformation to the aluminas ($\Delta l/l$, Table 3) is almost equal and about 3%. For the boehmite however, there is a small shrinkage of 1% in the direction of the *a* axis but an expansion of 6% in the direction of the *b* axis ($\Delta l/l$, Table 4). This strong anisotropy of the shrinkage is apparently the cause of the more pronounced tetragonal character of γ-alumina.

Formation of α- and θ-Al_2O_3

At high temperatures transformation to θ- and α-Al_2O_3 occurs. Pseudomorphosis does not occur any more; however a strong preferential orientation is found as for instance is shown in Figs. 10 and 15 for bayerite transformed into θ-Al_2O_3 at 980 °C. At a temperature of 750 °C the original cleavage plane is still clearly visible; at higher temperature the material of the particles is divided into small dumb-bell shaped microcrystallites.

Comparison of the crystallographic texture with the microporous texture

From nitrogen and lauric acid adsorption measurements it was shown (Lippens, 1961; de Boer & Lippens, 1964*a*, *b*) that during dehydration of the hydroxides slit-shaped pores with a width of 7 to 10 Å are formed. These pores are widened at higher temperatures and have disappeared above 750 °C.

For bayerite the shrinkage of the solid material in the direction of the *c* axis is more than 50%. However, the decrease of the granular volume is only about 16% as follows from nitrogen isotherms and electron microscope observations (de Boer, 1958). Therefore we may assume that the pores (and the lamellae of the solid material) are lying approximately perpendicular to the *c* axis of the original bayerite lattice, which is the [111] axis of the spinel. This means that the surface of the pores is formed by the (111) plane of the spinel which is the most stable plane. The same conclusion was drawn from the results of the adsorption of lauric acid on aluminas (de Boer, Houben, Lippens, Meijs & Walraven, 1962).

The number of narrow pores is very large, about 400 per μm. The thickness of the lamellae, which can be calculated from the specific volume and the surface area (Lippens, 1961; de Boer & Lippens, 1964*b*), is about 15 Å. The length of the unit cell of spinel in the [111] direction (perpendicular to the lamellae) is 13·7 Å. Consequently the strong disorder in the regular cubic *ABC* stacking is obviously also a result of the presence of the pores.

This lamellar character of the η-alumina skeleton hinders the diffusion of the Al atoms in the direction perpendicular to the lamellae. At a temperature of 750 °C the originally hardly perceptible pores are still clearly visible and the lamellae are still very thin (Fig. 16); at this temperature no recrystallization of the η-alumina into a more crystalline form is observed. The formation of θ-Al_2O_3 is accompanied by a complete recrystallization of the material (Fig. 15).

The lamellae of γ-alumina from boehmite are much thicker (100–150 Å); the few narrow pores disappear above 600 °C. On prolonged heating the formation of δ-Al_2O_3 can already be observed by X-ray diffrac-

Fig. 15. Bayerite particle after heating to 980 °C.

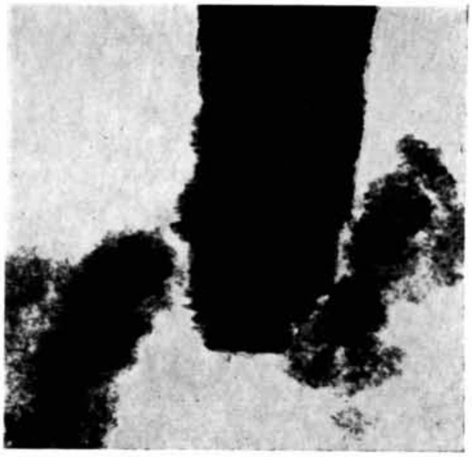

Fig. 16. Bayerite particle after heating to 750 °C.

tion. It must be noticed that in the case of gelatinous boehmite, which consists of very small fibrillar particles with a cross section of about 30 × 30 Å, the formation of the crystalline phase from the γ-alumina is hardly noticed at a temperature of 950 °C.

Discussion

From the observations mentioned above, the conclusion can be drawn that, besides the temperature, the pore system in the aluminas is a very important factor for the transformation of the disordered spinel-type η- or γ-alumina into the more crystalline phases.

The diffusion of the Al ions to their better ordered positions is brought to a halt by the surface of the pores. In η-alumina from bayerite with its numerous pores δ-Al_2O_3 therefore cannot be formed as it is in γ-alumina from crystalline boehmite.

Now the question arises why the number of pores in η-alumina is so much greater than in γ-alumina. Following the considerations of Sasvári & Zalai (1957) we may assume that the dehydration of the trihydroxides occurs through the loss of water from two OH groups in the same close-packed layer of OH groups forming one side of the cleavage plane, as the O–O distance in the layer (2·87 Å) is appreciably shorter than that across the cleavage plane (3·13 Å). To obtain the cubic close-packed *ABC* lattice the resulting layers have to shift, and this may be prevented by isolated OH groups still present on the surface.

In the case of boehmite these authors assume that the water molecules expelled arise from two OH groups *across* the cleavage plane, as their distance is only 2·47 Å, whereas the shortest distances between two OH groups in one side of the cleavage plane are 2·85 and 3·69 Å. At the same time the layers can slip in the direction of the hydrogen bonds, giving a cubic close-packing *CDCD* as described in this paper. This difference in dehydration mechanism may explain the difference in microporous texture of the spinel type aluminas and at the same time the differences in crystallographic texture.

That the diffusion of the Al ions is responsible for the recrystallization of the aluminas can be made clear by impregnating the spinel-type aluminas with a small quantity of Na_2O (1%). On heating, the Na ions are taken up in the lattice (they cannot be removed by treatment with dilute acids) and will occupy octahedral positions. Now the formation of the ordered spinel of δ-Al_2O_3 is completely inhibited, even at temperatures of 950 °C, whereas that of θ-Al_2O_3 (which contains about $\frac{3}{4}$ of the Al-atoms in tetrahedral positions (Saalfeld, 1960; Geller, 1960)) is facilitated.

We are greatly indebted to Prof. Dr W. G. Burgers (Department of Physical Chemistry, Technological University, Delft) for his helpful discussion on the interpretation of the X-ray and electron diffraction patterns and to Mr L. Moscou (Ketjen Research Laboratory, Amsterdam) for preparing the electron diffraction records.

References

Boer, J. H. de (1958). *The Shape of Capillaries* in Everett, D. H. & Stone, F. S., *The Structure and Properties of Porous Materials*. London: Butterworth.

Boer, J. H. de, Houben, G. M. M., Lippens, B. C., Meijs, W. H. & Walraven, W. (1962). *J. Catalysis*, **1**, 1.

Boer, J. H. de & Lippens, B. C. (1964*a*). *J. Catalysis*. **3**, 38, 44.

Boer, J. H. de & Lippens, B. C. (1964*b*). *J. Catalysis*. To be published.

Cowley, J. M. (1953). *Acta Cryst.* **6**, 53.

Cowley, J. M. & Rees, A. L. G. (1958). *Rep. Prog. Phys.* **21**, 165.

Geller, S. (1960). *J. Chem. Phys.* **33**, 676.

Jagodszinski, H. & Laves, F. (1948). *Schweiz. Miner. Petr. Mitt.* **28**, 456.

Kohlschütter, V., Beutler, W., Sprenger, L. & Berlin, M. (1931). *Helv. Chim. Acta*, **14**, 3.

Lippens, B. C. (1961). *Structure and Texture of Aluminas*. Thesis, Delft.

Moscou, L. & Vlies, G. van der (1959). *Kolloid-Z.* **163**, 35.

Oosterhout, G. W. van (1960). *Acta Cryst.* **13**, 932.

Oosterhout, G. W. van & Rooymans, C. J. M. (1958). *Nature, Lond.* **181**, 44.

Saalfeld, H. (1958). *Clay Min. Bull.* **3/19**, 249.

Saalfeld, H. (1960). *Neues Jb. Min., Abh.* **95**, 1.

Sasvári, K. & Zalai, A. (1957). *Acta Geol. Ac. Sci. Hung.* **4**, 415.

Schmäh, H. (1946). *Z. Naturforsch.* **1**, 323.

Tertian, R. & Papée, D. (1958). *J. Chim. Phys.* **55**, 341.

Watson, J. H. L., Parsons, J., Vallejo-Freire, A. & Santos, P. S. (1955). *Kolloid-Z.* **140**, 102.